

ORIGINAL PAPER

Open Access



# Investigation of mechanical properties and surface roughness of friction stir welded AA6061-T651

Rajesh Kumar Bhushan<sup>1\*</sup> and Deepak Sharma<sup>2</sup>

## Abstract

Friction stir welding (FSW) of 6-mm-thick plates of AA6061-T651 was carried out using a simple cylindrical pin tool. The impact of welding factors (rotational speed, welding speed) on tensile properties, microhardness, and surface roughness of FSW joints was investigated. Ultimate tensile strength (UTS), yield strength, and % elongation of AA6061-T651 base plate as well as FSW joints were found out using a universal testing machine (UTM). Maximum value of UTS and yield strength were achieved at rotational speed of 1400 rpm and welding speed of 20 mm/min. Minimum surface roughness was reached at rotational speeds of 1400 rpm and welding speed of 20 mm/min. Microstructural evolutions in the friction stir welded (FSWed) joint and microhardness profile were also determined. Maximum hardness of HV 120 was acquired for the stir zone (SZ). Hence, attainment of the maximum tensile strength, microhardness, and minimum surface roughness during FSW is a desired method to improve the service life and suitability of AA6061-T651.

**Keywords:** Friction stir welding, AA6061-T651, Tensile strength, Yield strength, Surface roughness

## Introduction

Working on a surface is affected by surface roughness. In most of the cases, failure of part starts on the surface. This is due to either incoherence or decline of the surface quality. Surface must be within limits of variations. The service qualities of the welded Al-alloy joints in the aerospace industry can be improved using FSW, which was initially used for welding difficult-to-weld high strength Al-alloys (Cam, Ipekoglu, & Tarik Serindag, 2014; Bhushan & Sharma, 2019). FSW is a solid-state welding process. FSW is also utilized to weld hollow objects, such as pipeline and containers. Components with three-dimensional profile are also joined using FSW. This technique is utilized to make butt, corner, lap, T, spot, and fillet junctions. The fracture of the welded joints under fluctuating loading conditions is initiated on the surface of the component. Hence, the

surface roughness significantly affects the fatigue of the welded joint.

As per Mishra and Ma (2005) in FSW a revolving tool with a specifically designed pin is placed into sides of plates to be joined. The tool then moves alongside the joint line, and plates are welded. According to Khaled (2005) when fastened joints are replaced with FSW joints, the result is weight and cost savings. Weight and cost savings are essential for aerospace industry. Weight savings are achieved due to the elimination of the fasteners. Cost savings are achieved because of a decrease in design, manufacturing, assembly, and maintenance time.

İpekoğlu, Erim, and Çam (2014) welded AA6061 plates in O and T6-temper state FSW in butt-position. After post-weld heat treatment, mechanical properties of FSW joints significantly improved with respect to as-welded plates and respective base plates. Cam et al., 2014 concluded that chemistry of dynamically recrystallized zone (DXZ) of AA6061-T6 joints

\* Correspondence: [rkbsmvdu@gmail.com](mailto:rkbsmvdu@gmail.com)

<sup>1</sup>Guru Ghasidas Vishwavidyalaya, Bilaspur, Chhattisgarh, India

Full list of author information is available at the end of the article

may be improved by utilizing high strength interlayer during FSW. This leads to substantial increase hardness of DXZ. He, Ling, and Li (2016) conducted FSW of AA6061 tick plates. They concluded that with rise in rotation speed, values of tensile longitudinal residual stresses enhanced marginally. Longitudinal tensile stresses were observed at the edge of the shoulder in AS of joints. Dorbane, Ayoub, Mansoor, Hamade, and Imad (2017) carried out FSW of AA6061 plates. Examination of samples showed that in temperature range of 25–200 °C locus of failure initiates at the region between thermomechanical-affected zones (TMAZ) and heat-affected zone (HAZ). However, at higher temperatures (300 °C), failure arises in stir zone. Zhou et al. (2019) carried out dual-rotation FSW of AA6061-T6. The impact of rotation speed on microstructure and mechanical properties of joints was examined. Defect-free joints were achieved under process parameters used.

This work is unique in the sense that research has been done about the microstructure and microhardness of FSW joints and to find out the value of process parameters to achieve best mechanical properties and minimum surface roughness of FSW joints of AA6061-T651, as this affects the corrosion behavior, fatigue strength, and life cycle of FSW joints. This research work has been carried at lower advance per revolution.

## Material and methods

### Workpiece material for FSW

AA6061-T651 sheet of size 1200 mm × 300 mm × 6 mm was identified for FSW. Plates were further cut into to size 100 mm × 50 mm × 6 mm. Press cutting machine was used for this. These workpieces are shown in Fig. 1.

Chemical composition of the AA6061-T651 plates was obtained using optical emission spectrometer. This is tabulated in Table 1.

### FSW machine

FSW was carried out on modified HMT-FN2V vertical milling machine. Special fixture was fabricated to grip plates in the desired location. Setup is displayed in Fig. 2.

### Fabrication of FSW tool

Tool geometry, tool size, and tool material are main criteria during FSW. Melting point and hardness of tool should be higher than the plates. Tool used in this work is shown in Fig. 3. Tool was manufactured from 25-mm diameter circular rod of high carbon high chromium D2 tool steel. Chemical composition of the high carbon high chromium D2 tool steel is tabulated in Table 2.

### Friction stir welding of AA6061-T651

Specimens to be joined using FSW were held on a specific fixture. This was done in order to stop the movements during the welding. A pilot hole of diameter 6 mm was drilled, at 10 mm from the last edge along the weld line. Due to this hole, tool easily plunged into the plates. Fixture was secured on table of milling machine. FSW tool was attached on collet of machine spindle. Spindle was rotated at required speed. Rotating tool pin moved into the plates till shoulder reached upper surface of plates. Length of tool pin was kept slightly shorter than thickness of plates. This is to prevent over plunging and tool breakage. Dwell time of 5 s was provided to the tool after the plunge. As a result of this, adequate frictional heat was generated. Tool moved forward along weld line at required welding speed. After welding was completed, tool was pulled out of plates 10 mm before reaching last edge of plates. Workpieces welded utilizing changed process parameters are displayed in Fig 4. Process parameters are tabulated in Table 3.

### Microstructure

Samples were selected from weld nugget. Samples were made ready for metallographic inspection using 220–320–500–1000 mesh emery papers. Then, polishing by with 2- $\mu$ m-sized diamond paste was done. Scanning electron



**Fig. 1** Test specimens of AA6061-T651

**Table 1** Composition of AA6061-T651

Cu	Mg	Si	Fe	Ni	Mn	Zn	Pb	Sn	Ti	Cr	Va	Al
0.211	1.18	0.810	0.321	0.013	0.068	0.169	0.010	0.003	0.061	0.046	< 0.01	97.09

microscope (SEM) attached with energy-dispersive spectroscopy (EDS) was used to study microstructure.

#### Microhardness

Vickers microhardness tester of maximum capacity 1000 gf was used for microhardness test. This is shown in Fig 5.

#### Tensile test

Ultimate tensile strength (UTS), yield strength, and % elongation of base metal and friction stir welded plates of AA6061-T651 were found out. Tensile test specimens were cut from AA6061-T651 and as-welded workpieces from the joint area, according to ASTM E8 standards. Electrical discharge machine (EDM) wire cut machine was utilized to cut specimens. Specimens were mounted on UTM, and load was applied until the specimen broke. In each tensile test, 03 specimens were used. Average value of 03 readings was taken.

#### Chemical composition test

Chemical compositions were obtained using vacuum optical emission spark spectrometer.

#### Surface roughness

There is a need to measure surface roughness because crack if any will start from the surface. Surface roughness of the AA6061-T651 and as-welded workpieces was measured using surface roughness tester. Surface roughness of the workpieces along the full length of the weld bead was measured.

#### Results

##### Chemical composition results

Composition of FSW joints was obtained using optical emission spectrometer. Results are given in Table 4. Optical emission spectrometry shows that the chemical composition of FSW joints is approximately same to that

**Fig. 2** Vertical milling machine HMT-FN2V



**Fig. 3** Fabricated FSW tool

of base alloy as reported in previous studies (Kafli & Nuran, 2009).

#### Microstructure-weld macrograph of FSW joint

Weld zones are the result of thermomechanical activities experienced by various areas of the weld. FSW joint consists of four zones: (a) base metal (BM); (b) HAZ, where plates are influenced only by heat and no plastic deformation occurs; (c) TMAZ, where plates are influenced by heat and plastic deformation; and (d) weld-nugget/stir zone (SZ). The SZ consists of noticeable onion ring structures. Onion rings are due to consecutive shearing of semi-cylindrical plastic material layers from front of the tool and their accumulation at back of the tool. Therefore, grain structure development in SZ is a very complicated mechanism. This is primarily because of continuous dynamic recrystallization (CDRX) and geometric dynamic recrystallization (GDRX). Particle-simulated nucleation (PSN) also shows minor role in certain cases.

The AA6061-T651 displays coarser elongated microstructure. In optical micrograph, grains are

oriented along rolling direction (Fig. 6(a)). Dark spots expose etch pits in microscope due to etching. Grains are equiaxed. Grains are somewhat oriented in rolling direction. Figure 6(b) shows microstructure of stir zone in advancing side. Elements are uniformly distributed in the microstructure. Therefore, FSW joint has sound microstructure. No microscopic cavities or flaws are detected at the weld nugget areas, so it can be said that thermal flow of material is uniform.

Analysis in Fig. 7 displays that main element at nugget zone are Al 97.52% and Si 0.84%.

#### Microhardness

Microhardness value of AA6061-T651 was 150 HV. The maximum hardness of HV 120 was achieved for SZ, while boundary between HAZ and TMAZ on advancing side showed hardness value of HV 81. A hardness loss was detected on advancing side (AS) and retreating side TMAZ region. Microhardness values of friction stir welded samples are tabulated in Table 5.

#### Relation between macrostructure and microhardness

Hardness distribution is not same in the weld area. It shows various FSW zones including SZ, TMAZ, and HAZ. The hardness of SZ is more than surrounding TMAZ and HAZ. Least microhardness is at boundary of HAZ and TMAZ on retreating side (RS). HAZ on advancing side (AS) likewise has a low hardness. This microhardness distribution is of “W” shape for precipitation strengthened alloy like AA6061 (Zhou et al., 2019). The external boundaries of this distribution would rise uninterruptedly in microhardness until it reaches natural plate hardness. According to Table 5, the SZ has maximum hardness equated with neighboring areas. It appears that comparatively high hardness of SZ is owing to its fine equiaxed grains and the associated grain boundary consolidation. Equiaxed grains result from dynamic recrystallization, while low hardness of TMAZ is a result of mixing of strengthening precipitates, which occurs due to high temperatures reached during FSW process. Low hardness of HAZ is as a consequence of grain coarsening and extra aging occurred in this zone.

#### Tensile test results

Tensile test results of AA6061-T651 and as-welded workpieces are shown in Table 6. Specimen nos. 1, 3, 5, and 7 were welded at welding speed of 16 mm/min. Specimen nos. 2, 4, 6, and 8 were welded at welding speed of 20 mm/min. Figure 8 shows change in UTS with variation in rotational speed, at constant welding speed of 16 mm/min. Figure 9 represents the change in UTS with variation in rotational speed, at constant welding speed of 20 mm/min. It was discovered from results that the maximum values of UTS and yield strength are obtained in FSW

**Table 2** Compositions of high carbon, high chromium grade D2

C	Mn	Si	S	Ni	Cr	Cu	V	W	Fe
2	0.3	0.3	0.03	0.3	4.88	0.25	1	1	Balance





**Fig. 4** Friction stir welded AA6061-T651 plates

specimen no. 8. The maximum value of UTS for FSW specimen no. 8 is 0.447 KN/mm<sup>2</sup>. These values were attained at a rotational speed of 1400 rpm and at a welding speed of 20 mm/min. UTS of as-welded specimens ranges from 68 to 80% of that of the base alloy. The minimum value of UTS was obtained at 900 rpm and 16 mm/min, for specimen no 3. The UTS and yield strength increase with increase in rotational speed for specimen no 2, 4, 6, and 8, at constant welding speed of 20 mm/min. Alike results were also obtained for breaking strength (BS), yield strength (YS) and % elongation. All tensile specimens had failed in heat-affected zone close to boundary of TMAZ. Specimens after tensile test are shown in Fig. 10.

**Surface roughness testing**

Effects of rotational speed on surface roughness of friction stir welded specimens were also investigated. Table 7 shows the surface roughness results of AA6061-T651FS welded specimens at different rotational speed (710–1400 rpm), at constant welding speed of 16 mm/min. As rotational speed decreases, roughness of the surface increases. Results discovered that smallest average surface roughness of 6.84 μm

was observed in specimen no. 8, i.e., at a rotational speed of 1400 rpm. The maximum average surface roughness of 9.07 μm was observed in specimen no. 3, i.e., at a rotational speed of 900 rpm. Surface finish of weld region of all the welded specimens is found to be good. Figure 11 shows the change in surface roughness with variation in rotational speed, at constant welding speed of 16 mm/min.

Table 8 shows surface roughness results of AA6061-T651FS welded specimens at different rotational speed (welding speed is maintained at 20 mm/min). As rotational speed decreases, roughness of surface enhances. Minimum average value of surface roughness of 6.71 μm was witnessed in specimen no. 8, i.e., at a rotational speed of 1400 rpm and constant welding speed of 20 mm/min. Minimum surface roughness of 6.71 μm was attained at rotational speed of 1400 rpm and at constant welding speed of 20 mm/min. Figure 12 signifies change in surface roughness with variation in rotational speed, while welding speed is constant at 20 mm/min. The high rotational speed results in less roughness due to high heat input.

**Table 3** FSW parameters

Specimen no.	Rotational speed (r/min)	Translation/welding speed (mm/min)
1	710	16
2	710	20
3	900	16
4	900	20
5	1120	16
6	1120	20
7	1400	16
8	1400	20

**Statistics**

**Statistics welding speed 16 mm/min**

Mean of UTS  $\bar{x} = \frac{\sum x}{n} = \frac{1430}{4} = 360$

Rotational speed (r/min)	UTS N/mm <sup>2</sup> (x <sub>i</sub> )	Deviation from mean $x_i - \bar{x}$	$(x_i - \bar{x})^2$
700	250	- 110	12,100
900	350	- 10	100
1120	400	40	1600
1400	430	70	4900
			18,700

Standard deviation =  $\sqrt{\frac{18700}{4}} = 68.37 \text{ N/mm}^2$



**Fig. 5** Vickers microhardness tester (maximum capacity 1000 gf)

**Statistics welding speed 20 mm/min**

Mean of UTS  $\bar{x} = \frac{\sum x}{n} = \frac{1610}{4} = 402$

Rotational speed (r/min)	UTS N/mm <sup>2</sup> ( $x_i$ )	Deviation from mean $x_i - \bar{x}$	$(x_i - \bar{x})^2$
700	370	- 32	1024
900	390	- 12	144
1120	410	8	64
1400	440	20	400
	1610		163

Standard deviation =  $\sqrt{\frac{1632}{4}} = 20.19 \text{ N/mm}^2$

**Statistics welding speed 16 mm/min**

Mean of surface roughness  $\bar{x} = \frac{\sum x}{n} = \frac{31.9}{4} = 7.98$

Rotational speed (r/min)	Surface roughness ( $\mu\text{m}$ ) ( $x_i$ )	Deviation from mean $x_i - \bar{x}$	$(x_i - \bar{x})^2$
700	9.07	1.09	1.19
900	8.41	0.43	0.19
1120	7.58	- 0.40	0.16
1400	6.84	- 1.14	1.3
	31.9		2.84

Standard deviation =  $\sqrt{\frac{2.84}{4}} = 0.84 \mu\text{m}$

**Statistics welding speed 20 mm/min**

Mean of surface roughness  $\bar{x} = \frac{\sum x}{n} = \frac{32.1}{4} = 8$

Rotational speed (r/min)	Surface roughness ( $\mu\text{m}$ ) ( $x_i$ )	Deviation from mean $x_i - \bar{x}$	$(x_i - \bar{x})^2$
700	8.9	0.90	0.81
900	8.87	0.87	0.76
1120	8.16	0.16	0.03
1400	6.17	1.83	3.35
	32.1		4.95

Standard deviation =  $\sqrt{\frac{4.95}{4}} = 1.11 \mu\text{m}$

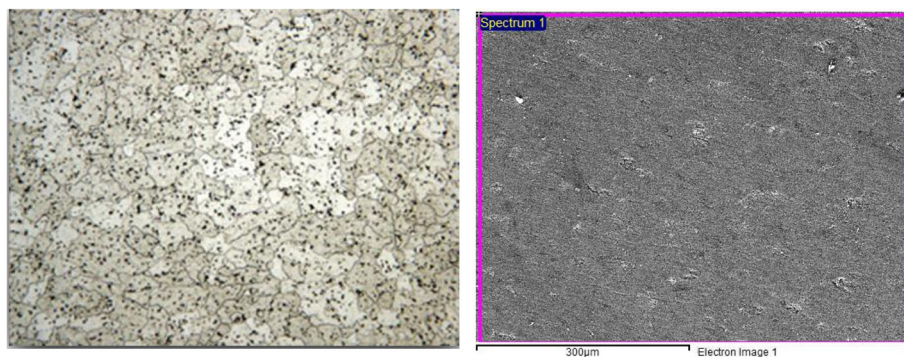
**Discussions**

**Microstructure aspects**

Sound FSW butt joints of AA6061 T651 specimens were obtained in this research work. This shows the distinctive capabilities of the FSW process. In FSW, the welding of plates is accomplished by generated heat due to rotation of tool on AA6061 T651 plates and plastic deformation. The generated heat is consumed in softening the plates. This facilitates the flow of material. During FSW, the material is shifted from AS to the RS at the front of the tool. Material is moved from RS to AS at rear end of the tool. When the material moves from AS, it forms an opening. When the tool rotates, the material from RS fills the opening created in the AS. This occurs if the amount

**Table 4** Chemical composition of friction stir welded AA6061-T651

Cu	Mg	Si	Fe	Ni	Mn	Zn	Pb	Sn	Ti	Cr	Va	Al
0.227	1.14	0.860	0.361	0.014	0.070	0.182	0.014	0.003	0.066	0.050	0.010	97.00



(a)AA 6061-T651

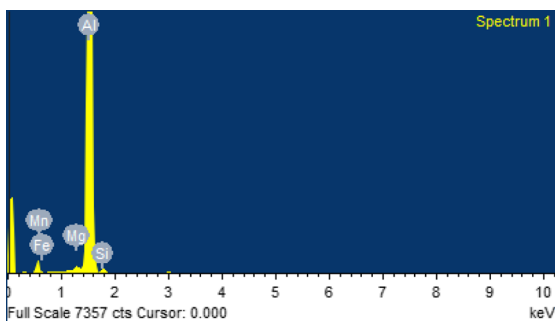
(b) AA 6061-T651 FSW joint

**Fig. 6** Microstructure of friction stir welded AA 6061-T651

of material moved to AS from RS is less than the amount of material removed from AS. If heat generated is less, plasticization of material will slow; this will lead to reduced flow of material. Result will be defect in the stir zone. Otherwise, if surplus heat is generated, turbulent flow of materials takes place. This leads to defects. Therefore, the optimal heat generation is required to attain the sound joint. Same is the opinion of Humphreys and Hatherly (2004). In spite of the optimal heat generated, the material is to be stirred by the pin shape. This is necessary to have sound joints. The area in touch with pin shoulder is the top part of stir section. This faced the effects such as heat generation and material flow. These are exclusively produced by rubbing of tool. Stirred zone comprises fine and equiaxed grains for both situations of FSW. Fine recrystallized zone at weld nugget is because of substantial plastic deformation. This is followed by dynamic recrystallization because of thermo-mechanical processing.

The SZ in AA6061 T651 has recrystallized grains with substantially minor grain size in contrast to BM. The grains on SZ of AA6061 T651 are considerably finer, in spite of the bigger original grain size of AA6061 T651. This is due to the happening of heavy plastic deformation

and robust dynamic recrystallization on the AA6061 T651. Similar were the observations of Murr, Liu, and McClure (1998). Al with FCC structure has additional slip planes present for distortion than Mg with HCP structure. This increases the tendency of Al to plastically deform. Hence, substantial grain modification witnessed in SZ of AA6061 T651 can be ascribed to major plastic deformation and subsequent heat input in AA6061 T651. Recrystallized microstructure in SZ would arise from a dynamic recovery (DRV) and a dynamic recrystallization (DRX). In rigorously deformed microstructure, subgrains are made by DRV and they create grains with HAGB in the process of DRX [Su, Nelson, & Sterling, 2005].The microstructures of the plates consists of coarse grains, a sufficient number of HAGBs, and large number of precipitates such as Mg<sub>2</sub>Si (for AA6061 T651). Hence, continuous grain growth (CGG) of dynamically recrystallized grains in stirred zone on AS is started. These grains are somewhat coarsened after plastic deformation. Reason is static annealing during weld cooling cycle. Distinctive boundary is there amid stirred zone and HAZ on the AS alike to results stated in previous articles [Kumar, Yuan, & Mishra, 2015; Venkateswarlu, Nageswararao, Mahapatra, Harsha, &



Element	Weight%	Atomic%
Mg K	0.87	0.97
Al K	97.52	97.91
Si K	0.84	0.74
Mn K	0.54	0.27
Fe K	0.22	0.11

**Fig. 7** EDX of FSW AA6061-T651 nugget

**Table 5** Microhardness of friction stir welded samples

Welded samples	Average microhardness (Hv)										
	Retreating side (RS)					Weld center	Advancing side(AS)				
	HAZ		TMAZ		NZ		NZ	TMAZ		HAZ	
15 mm	12 mm	9 mm	6 mm	3 mm	3 mm	6 mm	9 mm	12 mm	15 mm		
Friction stir welded AA6061-T651	80	89	96	103	110	120	112	105	98	90	81

**Table 6** Tensile test results of base alloy and as-welded specimens

	Base Alloy	Specimen 1	Specimen 2	Specimen 3	Specimen 4	Specimen 5	Specimen 6	Specimen 7	Specimen 8
Ultimate load	14.82	10.07	10.81	10.64	11.11	11.41	11.85	12.30	12.74
Breaking load	12.65	8.602	9.2	9.23	9.48	9.74	10.12	10.49	10.87
Yield load	14.22	9.66	10.38	10.46	10.66	10.94	11.37	11.80	12.22
UTS	0.52	0.35	0.37	0.35	0.39	0.40	0.41	0.43	0.447
BS	0.45	0.30	0.32	0.31	0.33	0.34	0.36	0.37	0.387
YS	0.50	0.34	0.36	0.34	0.37	0.38	0.40	.41	0.43
% Elongation	23.33	15.86	17.03	16.87	17.49	17.96	18.66	19.36	20.06

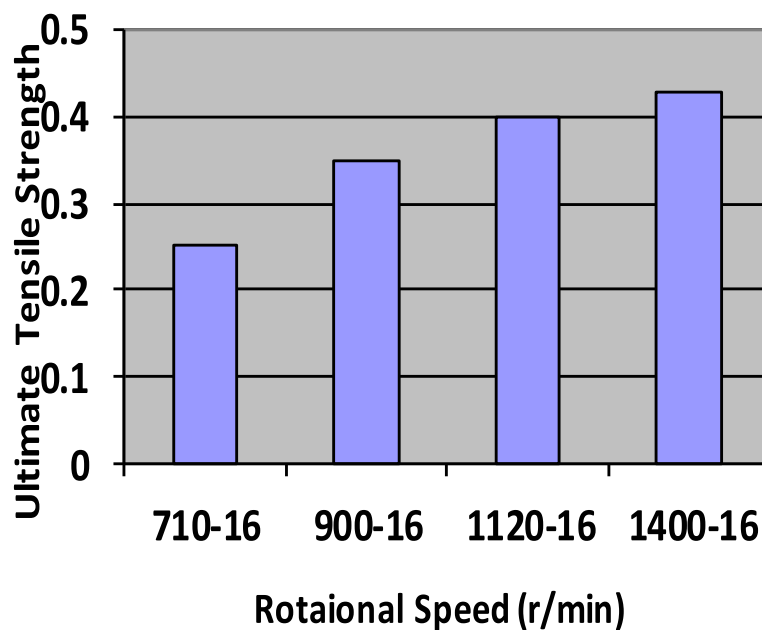


**Fig. 8** Rotational speed Vs tensile strength (welding speed 16 mm/min)



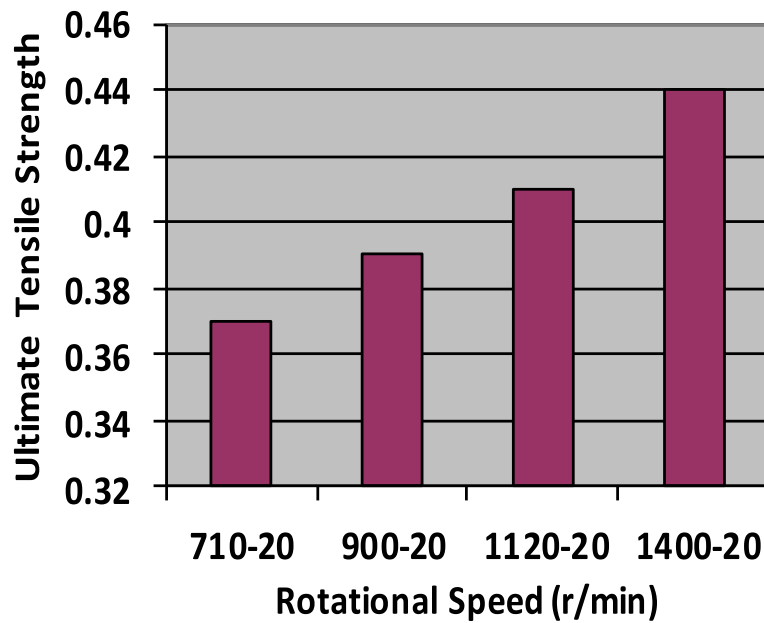


**Fig. 9** Rotational speed Vs tensile strength (welding speed 20 mm/min)

Mandal, 2015; Threadgill, Leonard, & Shercliff, 2009]. This is in difference with RS of weld joint. The boundary is further diffusive and rather unclear. Hence, the two zones cannot be easily differentiated. This occurs because strain rate and temperature gradients are much sharper on AS than that on RS. Shear plastic deformation in AA6061 T651 takes place within a lesser time. Reasons are the torsion and circumventing velocity fields with opposed directions in AA6061 T651.

**Surface roughness**





Surface roughness helps in deciding surface integrity. Roughness also helps in identifying function of surface. This is because an important share of material failure initiates at surface. It may be due to either the discontinuity

or deterioration of the quality of the surface. Surface finish also plays a significant role in corrosion resistance. Surface finish improves performance and reduces costs of life cycle of component. At the interface between the AA6061-T651 joints, onion rings are seen. Space between the layers in onion ring structure is equivalent to advancing motion of tool in single rotation. Therefore, it can be concluded that reduction in surface roughness of FSW joints has a significant role in governing the quality of FSW joints. Flow of material on AS is unlike from the flow on RS. AA6061-T651 on the RS certainly not go in rotational zone nearby the pin. The reason is that the material on the AS forms fluidized bed nearby pin and revolves around it. In transition zone, AA6061-T651 movement takes place mainly on the RS. This phenomenon is also supported by Li, Murr,



**Fig. 10** Specimens after tensile test

**Table 7** Surface roughness of aluminum alloy AA6061-T651 at different rotational speeds

Welding Parameters	FSW using 20 mm Shoulder Diameter	Surface Roughness(in $\mu\text{m}$ )
710 rpm 16 mm/min.		8.41
900 rpm 16 mm/min.		9.07
1120 rpm 16 mm/min.		7.58
1400 rpm 16 mm/min.		6.84

and McClure (1999). There is no flash on the RS. This is possibly owing to deficiency of heat generation triggered by decrease of surface roughness. Therefore, flexibility of AA6061-T651 reduces. Hence, it becomes difficult to extrude below the shoulder space. Width of the HAZ reduces steadily with the reduction in plate surface roughness. Reduction in FSW joint surface roughness leads to fall in the heat generation. Hence, less heat is transferred to HAZ region. This results in decrease in width of HAZ.

Amount of least FSW joint surface roughness shows the important influences on grain refinement. On one side, maximum grain size was attained with extreme FSW joint surface roughness. While on the other side, minimum grain size was attained with least FSW joint surface roughness. Therefore, it is inferred that grain size in NZ is reduced, when amount of AA6061-T651 surface roughness is reduced. Hirata et al. (2007) stated that grain size in NZ was reduced, when flow of friction

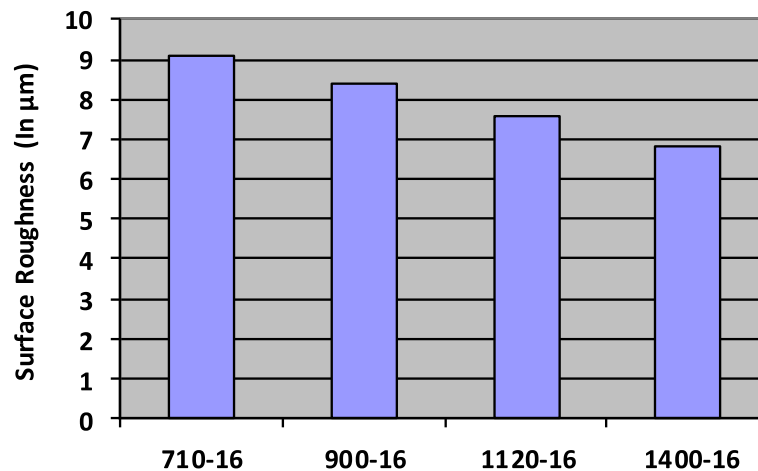


Fig. 11 Rotational Speed (rpm-mm/min)

heat was reduced. Therefore, the decrease in amount of plate surface roughness triggered the reduction in heat generation. This resulted in additional grain refinement.

#### Microhardness

Intermetallic formation, boundary energy, precipitate formation, and strain hardening of FSW joint affect the microhardness of joint. Extra hardness in SZ of FSW joints is due to the increase of grain boundaries and fine grains. Grain size is inversely proportional to hardness and strength. Hence, formation of fine recrystallized grains leads to increase in hardness in SZ. Similar results were also obtained by Guven and Cam et al. (2014). During welding, heat generated in SZ is transferred to neighboring regions (TMAZ and HAZ). For heat treatable AA6061 T651, strength and hardness mostly depend on availability and distribution of precipitates. Availability and distribution of precipitates in matrix are controlled by prevalent thermal conditions. Precipitation sequence of Al-Mg-Si 6xxx alloys is generally termed to be solid solution  $\rightarrow$ GP $\rightarrow$  $\beta''$  $\rightarrow$  $\beta'$  $\rightarrow$  $\beta$  (Mg<sub>2</sub>Si). During solutionization, precipitates are dissolved in matrix and form super saturated solid solution upon cooling. Further aging leads to precipitation of a secondary phase which reinforces strength of aluminum alloy [Gallais, Denquin, Bréchet, & Lapasset, 2008].

Because AA6061 T651 is heat treatable Al alloy, hardness is largely ascribed to existence of precipitates. Thermal cycle in TMAZ region makes dissolution of strengthening precipitates, which shows decreased hardness in retreating and advancing side in the Table 5. This region is softer since solute additions trapped in second phases dissolve back into solid solution. It can be also said that heating and cooling thermal condition exists in TMAZ, making precipitation dissolve in matrix. According to Cam et al. (2014), a hardness reduction



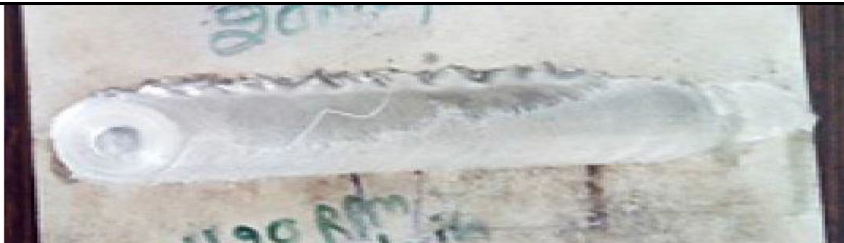

usually occurs in weld region of AA6061-T6 joints due to solution and/or coarsening of strengthening particles within TMAZ region and overaging in HAZ region. Scialpi, De Giorgi, De Filippis, Nobile, and Panella (2008) stated that HAZ has a peak temperature; therefore, results show decrease in hardness. The hardness of AA6061 T651 primarily is influenced by size and amount of precipitate particles. Maximum particles are mixed in TMAZ, and precipitates are partially mixed in stirred zone. Average grain size of TMAZ on AS was higher than that of SZ, whereas microhardness in SZ shows only a small enhancement as compared to that of TMAZ on AS. This is primarily because of existence of many precipitate particles in TMAZ. This outcome is in line with findings of Uzun, Dalle Donne, Argagnotto, Ghidini, and Gambaro (2005).

#### Tensile strength

Kim, Fujii, Tsumura, Komazaki, and Nakata (2006) stated that at constant rotational speed, mechanical opposition of joints increases with rise of travel speed. This is due to decreased heat input. Therefore, this research work considered less heat generation due to low welding speed. It is observed from Table 6 that UTS of all the 08 samples of FSW joints is less than the AA6061-T651 (BM). This is because of two reasons. First reason is influence of dissolved precipitates formed in FSW process. This results in decrease of tensile strength of joints. Second reason is robust tendency for intergranular cracking. This is as a consequence of the combination of weak grain boundaries and concentration of grain boundary stress. Therefore, cracks can propagate speedily along grain boundary. Hence, strength of the BM is higher than strength of welded joints. Ipekoglu and Cam et al. (2014) found that tensile strength of FSW joints were further less than lower



**Table 8** Surface roughness of AA6061-T651 at different rotational speeds

Welding Parameter	Surface Roughness using 20 mm Shoulder Diameter	Surface Roughness (In $\mu\text{m}$ )
710 rpm 20mm/min.		8.16
900 rpm 20mm/min.		8.90
1120 rpm 20mm/min.		8.87
1400 rpm 20mm/min.		6.71

strength of AA6061-T6 BM. Reason for this is coarsening of strengthening particles within DXZ and TMAZ regions and overaging in HAZ region. Increase in speed from 710 to 1400 rpm (at constant translation speed of 16 mm/min) linearly increases UTS from 0.25 to 0.43 kN/mm<sup>2</sup>, whereas increase in speed from 710 to 1400 rpm (at constant translation speed of 20 mm/min) linearly increases UTS from 0.37 to 0.44 kN/mm<sup>2</sup>. Increase in rotary speed increases heat input per unit weld length monotonically which leads to better bonding. This is the reason for increases in UTS with rise in

speed. No significant change is observed in UTS with increase of translation speed from 16 to 20 mm/min. Alike results were conveyed by Sharma, Dheerendra, and Pra-deep (2012).

**Conclusions**

This paper provides outcome of impact of welding parameters on tensile properties, microhardness, and surface roughness of friction stir welded AA6061-T651. Conclusions derived from this research work are:



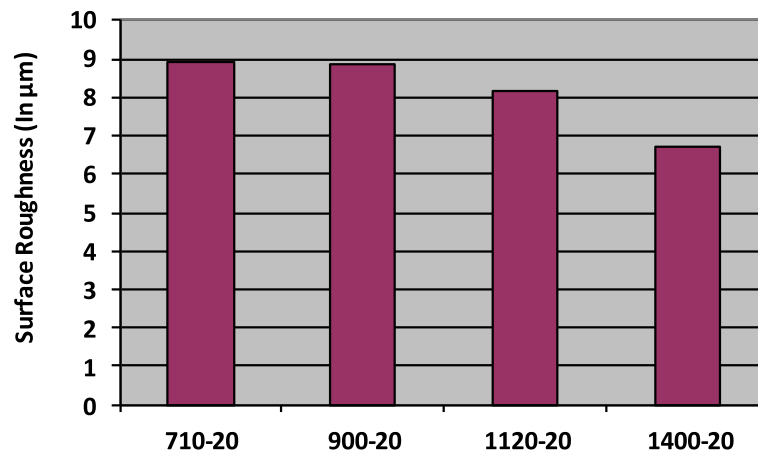


**Fig. 12** Rotational Speed (rpm-mm/min)

- UTS of as-welded specimens has reached up to 80% of that of base alloy. Maximum value of UTS and yield strength are found at rotational speed of 1400 rpm and welding speed of 20 mm/min.
- Result of surface roughness of the welded region showed that rotational speed has noteworthy effect on surface properties of welds. Surface roughness was minimum, at maximum rotational speeds, i.e., 1400 rpm, and welding speed of 20 mm/min.
- Microstructural analysis of FSW joint shows uniform distribution of particles.
- The maximum hardness of HV 120 was attained for SZ, while boundary between HAZ and TMAZ on advancing side exhibited lowest hardness value of HV 81.

#### Acknowledgements

Not applicable

#### Authors' contributions

Mr Deepak Sharma carried out the experimental work and prepared the paper. Dr Rajesh Kumar Bhushan checked and submitted the paper. The authors read and approved the final manuscript.

#### Funding

No funding was received for this research work

#### Availability of data and materials

All data generated or analyzed during this study are included in this published article.

#### Competing interests

There are no competing interests.

#### Author details

<sup>1</sup>Guru Ghasidas Vishwavidyalaya, Bilaspur, Chhattisgarh, India. <sup>2</sup>Shri Mata Vaishno Devi University, Katra, Jammu and Kashmir, India.

Received: 15 March 2020 Accepted: 20 May 2020

Published online: 06 June 2020

#### References

- Bhushan, Rajesh Kumar, Sharma, Deepak, Green welding for various similar and dissimilar metals and alloys: Present status and future possibilities, *Advanced Composites and Hybrid Materials*, 2019.
- Cam, G., Ipekoglu, G., & Tank Serindag, H. (2014). Effects of use of higher strength interlayer and external cooling on properties of friction stir welded AA6061-T6 joints. *Science and Technology of Welding and Joining*, 19(8), 715–720.
- Dorbane, A., Ayoub, G., Mansoor, B., Hamade, R. F., & Imad, A. (2017). Effect of temperature on microstructure and fracture mechanisms in friction stir welded Al6061 joints. *Journal of Materials Engineering and Performance*, 26-6, 2542–2554.
- Gallais, C., Denquin, A., Bréchet, Y., & Lapasset, G. (2008). Precipitation microstructures in an AA6056 aluminium alloy after friction stir welding: Characterisation and modeling [J]. *Materials Science and Engineering A*, 496, 77–89.
- He Jian & Ling Zemin, Li Huimin, (2016) Effect of tool rotational speed on residual stress, microstructure, and tensile properties of friction stir welded 6061-T6 aluminum alloy thick plate, *The International Journal of Advanced Manufacturing Technology*, 84,9-12:1953–1961.
- Hirata T, Oguri T, Hagino H, Tanaka T, Chung S.W, Takigawa Y, Higashi K, (2007) Influence of friction stir welding parameters on grain size and formability in 5083 aluminum alloy *Materials Science and Engineering: A*, 456: 344-349.
- Humphreys F, Hatherly M, (2004) *Recrystallization and related annealing phenomena*. 2nd ed. New York: Pergamon.
- İpekoğlu, Güven, Seçil Erim, and Gürel Çam, (2014) Investigation into the influence of post-weld heat treatment on the friction stir welded AA6061 Al-alloy plates with different temper conditions, *Metallurgical and Materials Transactions A*, 864(45a).
- Kafli H, Nuran A. Y. International Conference on Aerospace Sciences & Aviation Technology, 26 – 28 2009.
- Khaled T, (2005) An outsider looks at friction stir welding, Report, ANM 112 N-05-06.
- Kim, Y, Fujii, H, Tsumura, T, Komazaki, T, Nakata, K, (2006) Three defect types in friction stir welding of aluminum die casting alloy *Materials Science and Engineering: A*, 415: 250-254.
- Kumar, N., Yuan, W., & Mishra, R. S. (2015). *Friction stir welding of dissimilar alloys and materials* (1st ed.). Oxford, United Kingdom: Elsevier Science Ltd..
- Li, Y., Murr, L., & McClure, J. (1999). Flow visualization and residual microstructures associated with the friction-stir welding of 2024 aluminum to 6061 aluminum. *Materials Science and Engineering: A*, 271, 213–223.
- Mishra, R. S., & Ma, Z. Y. (2005). Friction stir welding and processing. *Mater Sci Eng R*, 50(1–2), 1–78.
- Murr, L. E., Liu, G., & McClure, J. C. (1998). ATEM study of precipitation and related microstructures in friction-stir-welded 6061 aluminium. *J. Mater Sci*, 33(5), 1243–1251.

- Scialpi, A., De Giorgi, M., De Filippis, L., Nobile, R., & Panella, F. (2008). Mechanical analysis of ultra-thin friction stir welding joined sheets with dissimilar and similar materials. *Materials & Design*, 29, 928–936.
- Sharma, C., Dheerendra, K. D., & Pradeep, K. (2012). Effect of welding parameters on microstructure and mechanical properties of friction stir welded joints of AA7039 aluminum alloy. *Materials and Design*, 36, 379–390.
- Su, J. Q., Nelson, T. W., & Sterling, C. J. (2005). Microstructure evolution during FSW/FSP of high strength aluminum alloys [J]. *Materials Science and Engineering A*, 405, 77–286.
- Threadgill, P. L., Leonard, A. J., & Shercliff, H. R. (2009). Withers P.J. Friction stir welding of alu-minium alloys. *Int Mater Rev*, 54, 49–93.
- Uzun H, Dalle Donne C, Argagnotto A, Ghidini T, Gambaro C, (2005) [Friction stir welding of dissimilar Al 6013-T4 To X5CrNi18-10 stainless steel](#) *Materials & design*,26:41-46.
- Venkateswarlu, D., Nageswararao, P., Mahapatra, M. M., Harsha, S. P., & Mandal, N. R. (2015). Processing and optimization of dissimilar friction stir welding of AA2219 and AA7039 alloys. *J Mater Eng Perform*, 24, 4809–4824.
- Zhou, L., Zhang, R. X., Hu, X. Y., Guo, N., Zhao, H. H., & Huang, Y. X. (2019). Effects of rotation speed of assisted shoulder on microstructure and mechanical properties of 6061-T6 aluminum alloy by dual-rotation friction stir welding. *The International Journal of Advanced Manufacturing Technology*, 100, 199–208.

### Publisher's Note

Springer Nature remains neutral with regard to jurisdictional claims in published maps and institutional affiliations.

Submit your manuscript to a SpringerOpen<sup>®</sup> journal and benefit from:

- ▶ Convenient online submission
- ▶ Rigorous peer review
- ▶ Open access: articles freely available online
- ▶ High visibility within the field
- ▶ Retaining the copyright to your article

---

Submit your next manuscript at ▶ [springeropen.com](https://www.springeropen.com)

---